



TITLE:

Ab initio lattice dynamics and phase transformations of ZrO₂

AUTHOR(S):

Kuwabara, A; Tohei, T; Yamamoto, T; Tanaka, I

CITATION:

Kuwabara, A ...[et al]. Ab initio lattice dynamics and phase transformations of ZrO₂. PHYSICAL REVIEW B 2005, 71(6): 064301.

ISSUE DATE:

2005-02

URL:

<http://hdl.handle.net/2433/39870>

RIGHT:

Copyright 2005 American Physical Society

Ab initio lattice dynamics and phase transformations of ZrO_2

Akihide Kuwabara,¹ Tetsuya Tohei,¹ Tomoyuki Yamamoto,² and Isao Tanaka¹

¹Department of Materials Science and Engineering, Kyoto University, Yoshida, Sakyo, Kyoto 606-8501, Japan

²Fukui Institute for Fundamental Chemistry, Kyoto University, Takano-Nishihiraki, Sakyo, Kyoto 606-8103, Japan

(Received 30 July 2004; published 9 February 2005)

Zirconia, ZrO_2 , is one of the most important ceramic materials in modern technology. Its versatility is closely related to phase transformations. Although the transformations have been repeatedly investigated by experiments, fundamental aspects of the transformations are still under debate. In the present paper, we have made first principles calculations to study the lattice dynamics of ZrO_2 polymorphs and phase transformation at finite temperatures. Cubic phase shows a soft mode at the X point in the Brillouin zone, which should spontaneously induce cubic-to-tetragonal transformation. In tetragonal and monoclinic ZrO_2 , all vibrational modes have real frequency. Calculations of Helmholtz free energies show that the tetragonal phase becomes more stable than the monoclinic phase above 1350 K, which is in quantitative agreement with experimental results. This confirms that vibrational entropy contributes to destabilize monoclinic ZrO_2 at elevated temperatures.

DOI: 10.1103/PhysRevB.71.064301

PACS number(s): 63.20.Dj, 63.70.+h, 65.40.-b, 71.20.Ps

I. INTRODUCTION

ZrO_2 has three polymorphs, cubic ($c\text{-ZrO}_2$), tetragonal ($t\text{-ZrO}_2$), and monoclinic ($m\text{-ZrO}_2$) phases. At elevated temperatures, ZrO_2 shows two kinds of solid-solid phase transformations, i.e., cubic-tetragonal ($c\text{-}t$) (Refs. 1 and 2) and tetragonal-monoclinic ($t\text{-}m$) (Refs. 3 and 4) transformations. The $c\text{-}t$ transformation is characterized by displacement of oxygen ion and elongation of cation sublattice in the $[001]$ and $[00\bar{1}]$ directions. The $t\text{-}m$ transformation occurs with a volume expansion and a shear distortion parallel to the basal plane of $t\text{-ZrO}_2$. ZrO_2 -based ceramics exhibits various outstanding properties that are closely related to the phase transformations. Alloying with suitable aliovalent cations stabilizes $c\text{-ZrO}_2$ at a room temperature and originates their functional properties such as high oxide-ionic conductivity.⁵ Cubic-stabilized ZrO_2 has been widely used as a solid electrolyte in a solid oxide fuel cell (SOFC) and an oxygen gas sensor. In 1975, Garvie *et al.*⁶ found the transformation toughening in $t\text{-ZrO}_2$ solid solutions. The large volume expansion associated with the $t \rightarrow m$ transformation is known as the origin of shielding force on crack propagation and thereby leads to high fracture toughness.⁷ In order to control and to improve the properties of ZrO_2 -based ceramics, it is necessary to fully understand the mechanism of these phase transformation. The phase transformation has been mainly analyzed through phenomenological approach. The $c\text{-}t$ transformation of ZrO_2 was first observed by Smith and Cline,⁸ and was originally considered as a first-order transformation.⁹⁻¹¹ On the other hand, Sakuma and co-workers proposed that the transformation was interpreted as a second-order type.^{12,13} Analyses from the Landau theory or the time-dependent Ginzburg-Landau (TDGL) equation have revealed that the $c \rightarrow t$ transformation can be explained by both of first-order^{14,15} and second-order models.^{16,17} Such phenomenological approaches have limitation to reveal the substance of phase transformation. The $t\text{-}m$ transformation is regarded as a martensitic transformation, for it has some

characteristics as a martensitic transformation, i.e., a large thermal hysteresis, an athermal transformation, a burst phenomenon, surface tilting, formation of twin and dislocation and an orientation relationship between the two phases.⁴

First principles calculations have been very successful to predict structures, properties, and behaviors of materials in a quantitative manner. Although most of the calculations have been done for the ground state, i.e., at the zero temperature, recent progresses in computational technique enable us to determine the full phonon dispersion of solids.¹⁸⁻²² Thereby one can compute specific heats, vibrational entropy, and other thermodynamical quantities as a function of temperature²³⁻³⁴ and can deal with phase transformation in finite temperatures or high pressures.³⁵⁻⁴⁰ However, such calculations are still in the early stage for applications to materials science issues, since they are still computationally demanding. The present study aims to clarify the origin of phase transformations in ZrO_2 by first principles lattice dynamics calculations.

II. COMPUTATIONAL METHODOLOGY

The structures of ZrO_2 polymorphs were preliminarily determined by ground state calculations. The total energy calculations were performed using VASP code,^{41,42} which is based on the density functional theory (DFT).⁴³ Exchange and correlation functional was given by the generalized gradient approximation (GGA) as proposed by Perdew and Wang.⁴⁴ Electron-ion interaction was represented by the projector augmented wave (PAW) method⁴⁵ with plane waves up to an energy of 500 eV. The reference configurations for valence electrons were $4s^2 4p^6 5s^2 4d^2$ for Zr and $2s^2 2p^4$ for O. Lattice constants and internal positions in primitive cells at various volumes were fully optimized. The \mathbf{k} -point meshes of Brillouin zone sampling in primitive cells, based on the Monkhorst-Pack scheme,⁴⁶ were $4 \times 4 \times 4$ for cubic ($c\text{-ZrO}_2$, 10 irreducible points), $5 \times 5 \times 3$ for tetragonal ($t\text{-ZrO}_2$, 12 irreducible points) and $3 \times 3 \times 3$ for monoclinic

TABLE I. Calculated structural parameters of a unit cell and total energy per formula unit for *c*-, *t*-, and *m*-ZrO₂ in comparison with a previous pseudopotential calculation and with an experiment.

<i>c</i> -ZrO ₂ (<i>Fm</i> 3 <i>m</i>)	Present	Calc. ^a	Expt. ^b
<i>a</i> (Å)	5.145	5.0371	5.108
Energy (eV/f.u.)	-28.413		
<i>t</i> -ZrO ₂ (<i>P</i> 4 ₂ / <i>nmc</i>)	Present	Calc. ^a	Expt. ^c
<i>a</i> (Å)	3.642	3.5567	3.591
<i>c</i> (Å)	5.295	5.1044	5.169
<i>c</i> /√2 <i>a</i>	1.028	1.0140	1.018
O(0, 0.5, <i>z</i>)	0.196	0.2082	0.204
Energy (eV/f.u.)	-28.503		
<i>m</i> -ZrO ₂ (<i>P</i> 2 ₁ / <i>c</i>)	Present	Calc. ^a	Expt. ^d
<i>a</i> (Å)	5.211	5.1083	5.1505
<i>b</i> (Å)	5.286	5.1695	5.2116
<i>c</i> (Å)	5.388	5.2717	5.3173
β (deg)	99.590	99.21	99.230
Zr1(<i>x</i> , <i>y</i> , <i>z</i>)	(0.277, 0.043, 0.210)	(0.2769, 0.0422, 0.2097)	(0.2754, 0.0395, 0.2083)
O1(<i>x</i> , <i>y</i> , <i>z</i>)	(0.070, 0.336, 0.343)	(0.0689, 0.3333, 0.3445)	(0.0700, 0.3317, 0.3447)
O2(<i>x</i> , <i>y</i> , <i>z</i>)	(0.450, 0.758, 0.478)	(0.4495, 0.7573, 0.4798)	(0.4496, 0.7569, 0.4792)
Energy (eV/f.u.)	-28.612		

^aReference 47.

^bCalculated from cubic root of the (√2*a*)² × *c* of *t*-ZrO₂ unit cell in Ref. 48.

^cReference 48.

^dReference 49.

(*m*-ZrO₂, 10 irreducible points) in order to obtain absolute energy convergence ≤1 meV/atom. Dynamical properties were obtained from the direct method.²² In this method, phonon frequencies were calculated from Hellmann-Feynman (HF) forces generated by nonequivalent atomic displacement in a supercell for a crystal structure. In the present study, the dimensions of supercells were 2 × 2 × 2, 3 × 3 × 2, and 2 × 2 × 2 of their unit cells for monoclinic, tetragonal, and cubic structures, respectively. For the calculation of those large systems, **k**-point sampling is limited to 2 × 2 × 2. A dynamical matrix was constructed from HF forces acting on all atoms in supercells with a displaced atom, and phonon frequencies were calculated by solving the eigenvalue problem for the dynamical matrix. Thermal expansion is indirectly taken into account through calculations for various lattice volumes. Born effective charges^{18,19} were not included in our calculation. Therefore, longitudinal optical/transverse optical (LO/TO) splitting at Γ point were not obtained in the present study. However, experimental specific heat and other thermodynamical parameters can be well reproduced without the LO/TO splitting as will be mentioned later.

III. RESULTS AND DISCUSSION

A. Atomic structure and static energy

The optimized lattice constants, internal atomic positions in Wyckoff notation and the total energy per formula unit of

ZrO₂ polymorphs at the ground state are presented in Table I together with previous theoretical and experimental reports. It can be seen that the present results are in good agreement with experimental data within the usual accuracy of GGA calculations. As shown in Table I, the energetic hierarchy of ZrO₂ polymorphs is $E_{\text{cubic}} > E_{\text{tetragonal}} > E_{\text{monoclinic}}$. Our ground state calculations precisely reproduce the phase stability of ZrO₂ at the ambient temperatures.

B. Lattice dynamics

First principles calculations of phonon in ZrO₂ have been reported by some groups. Parlinski *et al.*²² and Detraux *et al.*⁵⁰ have pointed out the presence of soft mode in *c*-ZrO₂. The dielectric properties of ZrO₂ polymorphs were examined by Rignanese *et al.*⁵¹ and Zhao and Vanderbilt.⁴⁷ However, no reports have been available for the phase transformations in ZrO₂. Figure 1 shows dispersion curves and density of states of phonon (phonon-DOS) in ZrO₂. Similar to the previous works, the present study also shows that *c*-ZrO₂ has a phonon with imaginary frequency (6.4i THz) at the *X* point. Recent first principles and semiempirical calculations have obtained the same soft mode.^{22,50,52} This soft mode (X_2^-) at the Brillouin zone boundary should result in transformation from cubic to tetragonal phase. On the other hands, all modes of *t*-ZrO₂ have real frequency. The X_2^- mode of *c*-ZrO₂ changes into A_{1g} mode at Γ point of *t*-ZrO₂ which has real frequency (8.7 THz). In contrast to the cubic phase, the

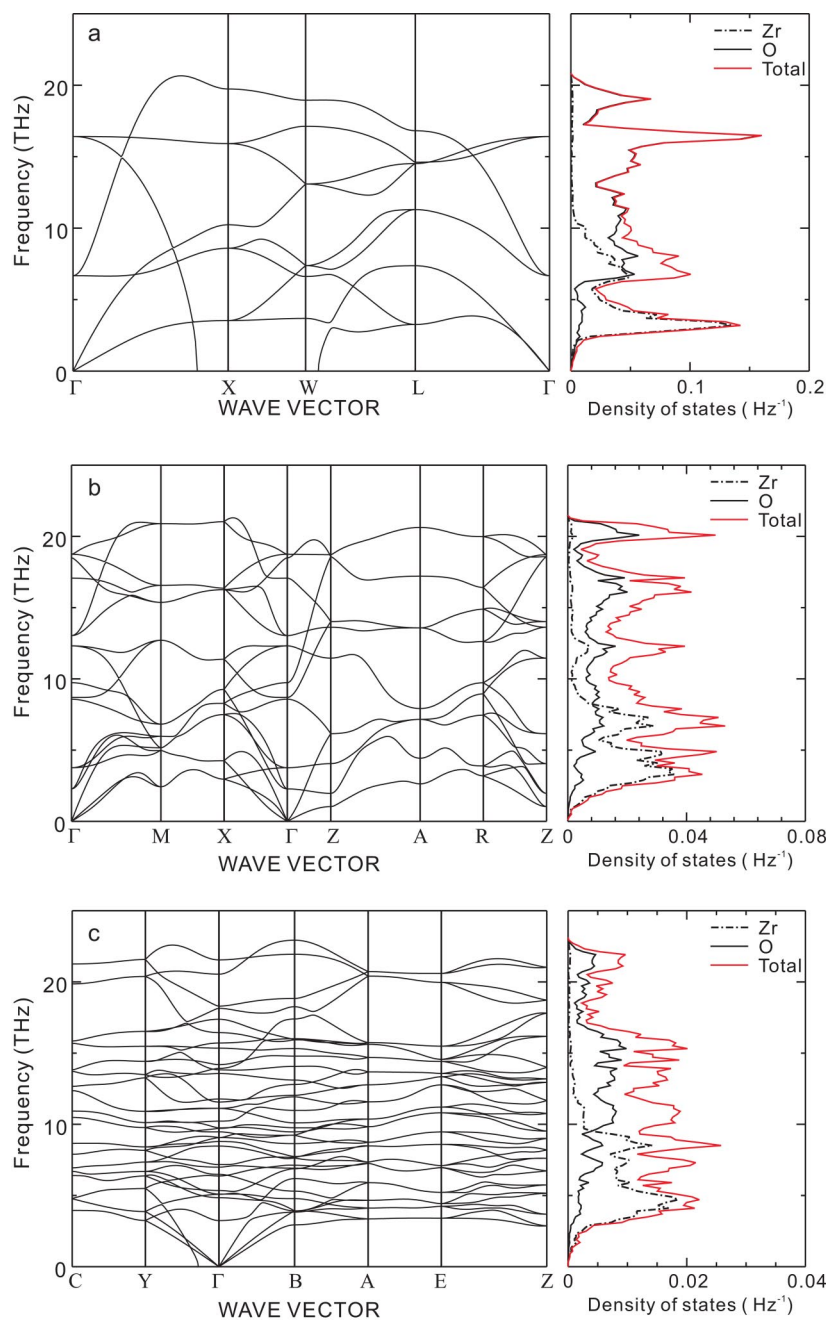


FIG. 1. (Color online) Dispersion curves of phonon and phonon-DOS in (a) cubic, (b) tetragonal, and (c) monoclinic phases. Partial phonon-DOS of constituent elements per atom are also shown.

tetragonal phase is a stable structure with regard to the lattice vibration. Dispersion curve of the phonon of *m*-ZrO₂ is composed of real frequency except that imaginary frequency of the transverse acoustic (TA) mode at the vicinity of Γ point along the ΓY line. The direct method occasionally obtains unexpected softening of long wavelength phonon owing to the limitation of supercell size.⁵³ Such problem can be resolved by sufficiently larger supercell. However, it should be noted that this error is small (0.7i THz). Figure 1 also shows phonon-DOS of three phases in the ground state and their partial components per atom. Since a zirconium atom is heavier than an oxygen atom, partial phonon-DOS indicates that oxygen has higher frequencies than zirconium in all phases. In the cubic phase, the phonon-DOS of zirconium atoms mainly distributes below 10 THz and has a sharp peak

at 3.2 THz. The spectrum of oxygen atoms exists higher than 5 THz and has large peaks at 16.5 and 19.0 THz. In the spectra of *t*-ZrO₂, discriminative peaks disperse and become smaller compared with those of *c*-ZrO₂. *m*-ZrO₂ has much broader phonon-DOS spectra and has no remarkably strong peaks. The frequency of phonon scatters with lowering symmetry.

Lattice vibration at Γ point can be closely investigated by infrared (IR) and Raman spectra. To our knowledge, no experimental IR and Raman spectra of pure *c*-ZrO₂ is reported thus far. Therefore, discussion on the phonon at Γ point is limited to *t*- and *m*-ZrO₂ here. Group theoretical analysis indicates that *t*-ZrO₂ has three IR-active modes ($2E_u + A_{2u}$) and six Raman-active modes ($3E_g + A_{1g} + 2B_{1g}$). In the case of *m*-ZrO₂, 15 IR-active modes ($8A_u + 7B_u$) and 18 Raman-

TABLE II. Frequencies (cm^{-1}) and symmetry assignment of IR-active phonon mode at Γ point in t - and m -ZrO₂. Parentheses indicate the different symmetry assignment proposed in the literatures from the present results. “(u)” means that the assignment is unidentified.

t -ZrO ₂					
Present study	Calc. ^a	Calc. ^b	Calc. ^c	Expt. ^d	
76	E_u	154	152.7	146	164
			270.5 (LO)		232 (LO)
325	A_{2u}	334	338.5	274	339
			663.8 (LO)		354 (LO)
435	E_u	437	449.4	446	467
			734.1 (LO)		650 (LO)
m -ZrO ₂					
Present study	Calc. ^a	Calc. ^c	Expt. ^e	Expt. ^f	
170	A_u	181 (B_u)	192		
212	B_u	224 (A_u)	227	224 (A_u)	220 (A_u)
233	A_u	242	229		
239	A_u	253 (B_u)	294 (B_u)	257	250
283	B_u	305 (A_u)	309 (A_u)		
303	B_u	319	332	324 (u)	330
325	A_u	347	346 (B_u)	351 (B_u)	
341	B_u	355	347 (A_u)	376	360
386	A_u	401	377 (B_u)	417	420
393	B_u	414	450 (A_u)	453 (A_u)	440 (A_u)
461	A_u	478	544	511 (B_u)	510 (B_u)
464	B_u	483	578		540
548	A_u	571	597	588 (B_u)	590 (B_u)
				687 (u)	610 (B_u)
610	A_u	634	712	725 (u)	730
685	B_u	711	745	789	750

^aReference 47.

^bReference 51.

^cReference 54.

^dReference 55.

^eReference 56.

^fReference 57.

active modes ($9A_g+9B_g$) exist. The calculated frequencies of IR- and Raman-active mode at Γ point in t - and m -ZrO₂ are tabulated in Tables II and III, respectively, in comparison with previous theoretical and experimental results. The present study cannot obtain the frequencies of IR-active LO modes, for the Born effective charges were not considered. The frequency of lower E_u mode of t -ZrO₂ is underestimated half as much as the previous reports. Except these points, our calculations well reproduce the experimental IR spectra of t -ZrO₂. As is the case with Ref. 47 and 54, calculated IR-active modes in m -ZrO₂ show clear deference from experimental ones. Although theoretical calculations obtain phonons with frequencies of around 180, 230, and 300 cm^{-1} , the peaks of equivalent modes have not been reported in experimental spectra.^{56,57} Zhao and Vanderbilt⁴⁷ calculated the intensity of an IR spectrum for m -ZrO₂. They have found that the peak intensities of these modes are very weak and have proposed that these peaks are probably obscured by

TABLE III. Frequencies (cm^{-1}) and symmetry assignment of Raman-active phonon mode at Γ point in t - and m -ZrO₂. Parentheses indicate the different symmetry assignment proposed in the literatures from the present results. “(u)” means that the assignment is unidentified.

t -ZrO ₂					
Present study	Calc. ^a	Calc. ^b	Expt. ^c	Expt. ^d	Expt. ^e
126	E_g	146.7	191	146	149
286	B_{1g}	259.1 (A_{1g})	242	318	269 (E_g)
290	A_{1g}	330.5 (B_{1g})	282	270	319 (B_{1g})
411	E_g	473.7	483	458	461
569	B_{1g}	607.0	589	602	602 (A_{1g})
625	E_g	659.2	659	648	648 (B_{1g})
m -ZrO ₂					
Present study	Calc. ^f	Calc. ^b	Expt. ^g	Expt. ^{h,i}	Expt. ^j
108	A_g	103	130	102	99
162	B_g	175	194 (A_g)	179	177
169	A_g	180	216 (B_g)	179	
179	A_g	190	223	190	189
216	B_g	224	224	224	222
			260 (A_g)	270 (u)	270
293	A_g	313 (B_g)			
303	B_g	317 (A_g)	296	305 (A_g)	305
316	B_g	330	307 (A_g)	334	331
324	A_g	345	348	348	343
371	B_g	381 (A_g)	407	381	376
371	A_g	382 (B_g)	433	385 (u)	376
453	A_g	466	503	476	473
473	B_g	489		505	498
512	B_g	533	568	536	534
524	A_g	548	616	556	557
580	B_g	601	602	616	613
605	A_g	631	680	637	633
			686 (B_g)		705
719	B_g	748	769	757	780

^aReference 51.

^bReference 54.

^cReference 58.

^dReference 59.

^eReference 60.

^fReference 47.

^gReference 61.

^hReference 62.

ⁱSymmetry assignment is not proposed.

^jReference 63.

strong ones existing near. As can be seen in Table III, our calculations of Raman-active modes in both t - and m -ZrO₂ are in good agreement with the data of the literature. The correspondence between the present results and the previous experiments for IR and Raman spectra implies that our calculations on lattice dynamics are suitable to analyze the thermodynamical properties of ZrO₂ polymorphs.

C. Thermodynamical properties and phase transformation

Based on quasiharmonic approximation, we can obtain Helmholtz free energy (F), entropy of vibration (S_{vib}), and

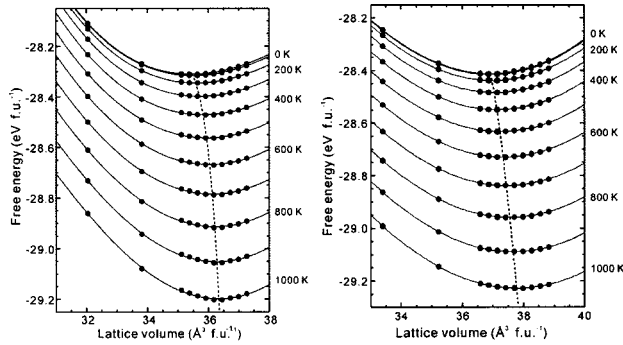


FIG. 2. Plots of Helmholtz free energy (F) per formula unit against lattice volume (V) per formula unit in (a) tetragonal and (b) monoclinic phases from 0 to 1000 K at every 100 K. Solid lines are F - V fitting curves according to the third-order Birch-Murnaghan equation of states. Dashed line connects minimum energy points at each temperature.

specific heat at constant volume (C_V) at finite temperature from phonon-DOS with various lattice volumes (V).⁶⁴ Application of the quasiharmonic approximation to c - ZrO_2 was impracticable because density of soft modes remarkably increases even with small volume expansion of about 0.7%. We will hereafter discuss only t - and m - ZrO_2 . Figure 2 shows a plot of the Helmholtz free energy of t - and m - ZrO_2 against a lattice volume at temperatures from 0 to 1000 K. A lattice volume with minimum free energy was determined from fitting curves of the third-order Birch-Murnaghan equation of states⁶⁵ at each temperature under the condition of $\partial B/\partial P=4$ where B and P is isothermal bulk modulus and pressure, respectively. Minimum energy points are connected by a dashed line in Fig. 2. As shown in this figure, the lattice volume becomes larger with increase of temperature. Thermal volume expansion can be indirectly reproduced by the quasiharmonic approximation without taking anharmonicity into account. Figure 3 shows the temperature dependence of volume expansion ($\delta V/V$), isothermal

bulk modulus (B), molar specific heat at constant volume (C_V) and that at constant pressure (C_P) and entropy (S) of m - ZrO_2 . Experimental results are also indicated in this figure. $\delta V/V$ was defined as

$$\delta V/V = \frac{V(T) - V(300)}{V(300)}, \quad (1)$$

where $V(T)$ is a lattice volume at a given temperature of T . Bulk modulus can be obtained from the F - V fitting curve according to the third-order Birch-Murnaghan equation of states as shown in Fig. 2. Lattice dynamics calculation with quasi-harmonic approximation can directly calculate C_V , but not C_P because of volume-fixed calculation. Alternatively, C_P can be evaluated using a thermodynamical relationship between C_V and C_P such as $C_P - C_V = \alpha^2 V B T$, where α is thermal expansivity expressed as

$$\alpha = \frac{1}{V} \left[\frac{\partial V}{\partial T} \right]_P. \quad (2)$$

As indicated in Fig. 3, our calculations are in good agreement with experimental data of $\delta V/V$, C_P and S . Softening of B with temperature can be observed. Chan *et al.*⁶⁶ reported B of 201 and 192 GPa at 293 K and 1273 K for m - ZrO_2 , respectively, using sound velocity measurements. The present calculations underestimated the experimental B . This is, however, a general trend for calculation with the GGA. These results imply that the temperature dependence of these physical parameters can be satisfactorily evaluated without taking into account the influence of Born effective charges. This is probably due to that total phonon-DOS, from which thermodynamical functions are calculated,⁶⁴ is impervious to LO/TO splitting. Born effective charge only affects the frequencies of LO modes with long wavelength and leave the frequencies of TO modes invariant. Therefore, LO/TO splitting contributes little to the total phonon-DOS because the influence of LO modes is limited only to the small volume of a reciprocal lattice in the vicinity of the Γ point.⁶⁷

The t - m phase transformation of ZrO_2 has been accepted as a typical martensitic transformation in ceramics and exhibits a thermal hysteresis. The temperatures of the t - m transformation on cooling (M_s) and heating (A_s) were reported to be about 1200 K and 1500 K, respectively.^{3,4} The transformation temperature determined from Gibbs free energies should exist between M_s and A_s because the transformation needs driving force to overcome strain energy and interface energy induced by the transformation. Comparing the temperature-dependent free energies of the t and m phases, we are able to obtain the transformation temperature. Solid-solid phase transformation can be discussed with Helmholtz free energy instead of Gibbs free energy in an ambient pressure because volume change (ΔV) is very small. Given that P is 1 atm, the calculated value of $P\Delta V$ for t - and m - ZrO_2 is 6.9×10^{-7} eV at 300 K. The effect of $P\Delta V$ is thus negligible. Figure 4(a) indicates plots of difference of Helmholtz free energy (ΔF_{t-m}), internal energy (ΔU_{t-m}), and entropy term ($T\Delta S_{t-m}$) against temperature. It can be clearly found from Fig. 4(a) that the calculated temperature of t - m phase transformation is about 1350 K. This is consistent with the pre-

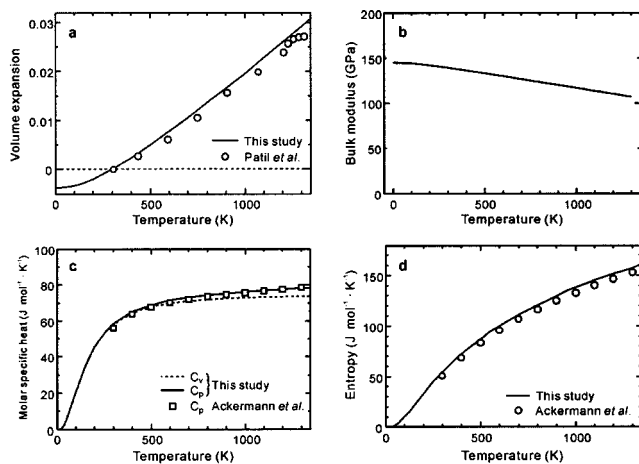


FIG. 3. Plots of (a) volume expansion ($\delta V/V$), (b) bulk modulus (B), (c) molar specific heat at constant volume (C_V) and that at constant pressure (C_P), and (d) entropy (S) against temperature in m - ZrO_2 . Solid lines are the calculated results and blank symbols are experimental results quoted from Refs. 1 and 3.

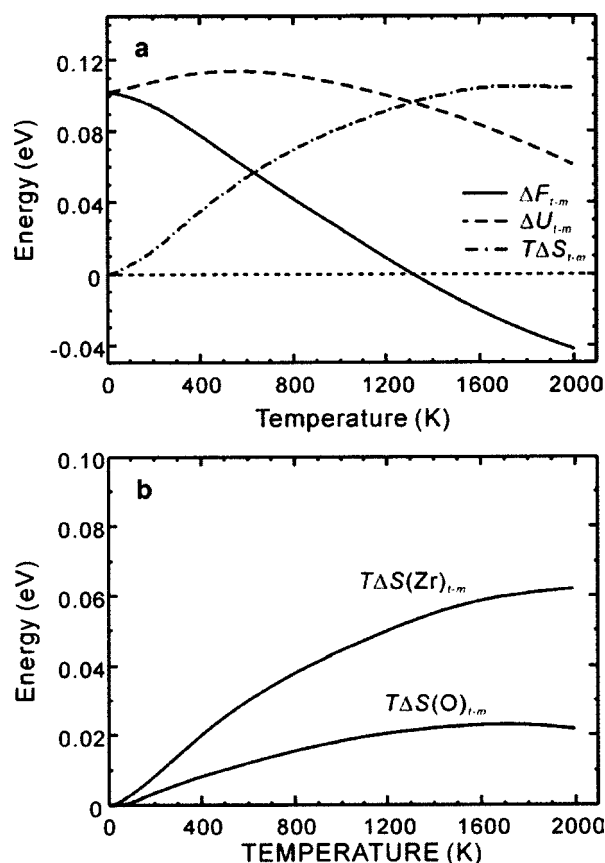


FIG. 4. (a) Temperature dependence of difference of Helmholtz free energy (ΔF_{t-m}), internal energy (ΔU_{t-m}), and entropy term ($T\Delta S_{t-m}$) between *t* and *m* phases. Energies per formula unit are indicated. (b) Partial component of $T\Delta S_{t-m}$ for zirconium and oxygen per atom are plotted against temperature.

diction that the energetical transformation temperature is between experimental M_s and A_s . To our best knowledge, the *t-m* transformation temperature of ZrO_2 can be quantitatively reproduced for the first time without any empirical parameters. *t-ZrO*₂ is less stable than *m-ZrO*₂ with the regard to the internal energy over the whole range of temperature. On the other hand, the $T\Delta S_{t-m}$ of *t-ZrO*₂ is always larger than that of

*m-ZrO*₂. This is due to the fact that S_{vib} of *t-ZrO*₂ is always larger than that of *m-ZrO*₂. Contributions of zirconium and oxygen atoms to $T\Delta S_{t-m}$ are shown in Fig. 4(b). Both elements in *t-ZrO*₂ have larger vibrational entropy than those in *m-ZrO*₂. It can be concluded that inversion of free energy between *t*- and *m-ZrO*₂ at elevated temperatures is originated from the effect of vibration. These results suggest that *ab initio* calculations for lattice dynamics on the basis of the quasiharmonic approximation are powerful tools to theoretically investigate solid-solid phase transformation in a quantitative manner.

IV. CONCLUSION

Phonon vibrations and their density of states in *c*-, *t*-, and *m-ZrO*₂ were systematically investigated by first principles calculations using VASP code combined with the direct method. In *c-ZrO*₂, the frequency of X_2^- mode was calculated to be imaginary. This unstable soft-mode should induce *c*→*t* phase transformation. On the other hand, it was found that the phonon modes have real frequencies in *t*- and *m-ZrO*₂ and are observed to be stable vibrations.

Based on the quasiharmonic approximation, temperature dependence of Helmholtz free energies of *t*- and *m-ZrO*₂ was computed. Our calculations indicated that *t-ZrO*₂ become more stable than *m-ZrO*₂ at temperatures higher than 1350 K. The calculated temperature of *t-m* phase transformation is in quantitatively good agreement with experimental data. Further investigation reveals that vibrational entropy of Zr and O ions is attributed to the stabilization of *t-ZrO*₂ at elevated temperatures. Phonon is one of the principal factors to control *c-t-m* phase transformation in ZrO_2 .

ACKNOWLEDGMENTS

This work is supported by three projects from the Ministry of Education, Culture, Sports, Science and Technology of Japan. They are a Grant-in-Aid for Scientific Research on Priority Areas (No. 751), the Computational Materials Science Project in Kyoto University and the 21st century COE program.

- ¹R. J. Ackermann, E. G. Rauh, and C. A. Alexander, *High. Temp. Sci.* **7**, 304 (1975).
- ²P. Aldebert and J. P. Traverse, *J. Am. Ceram. Soc.* **68**, 34 (1985).
- ³R. N. Patil and E. C. Subbarao, *J. Appl. Crystallogr.* **2**, 281 (1969).
- ⁴E. C. Subbarao, H. S. Maiti, and K. K. Srivastava, *Phys. Status Solidi A* **21**, 9 (1974).
- ⁵T. H. Etsell and S. N. Flengas, *Chem. Rev. (Washington, D.C.)* **70**, 339 (1970).
- ⁶R. C. Garvie, R. H. J. Hannink, and R. T. Pascoe, *Nature (London)* **258**, 703 (1975).
- ⁷R. H. J. Hannink, M. K. Patrick, B. C. Muddle, *J. Am. Ceram. Soc.* **83**, 461 (2000).

- ⁸D. K. Smith and C. F. Cline, *J. Am. Ceram. Soc.* **45**, 549 (1962).
- ⁹I. Cohen and B. E. Schaner, *J. Nucl. Mater.* **9**, 18 (1963).
- ¹⁰C. A. Andersson, J. Gregg, Jr., and T. K. Gupta, in *Advances in Ceramics Vol. 12 Science and Technology of Zirconia II*, edited by N. Claussen, M. Rühle, and A. H. Heuer (American Ceramic Society, OH, 1984), pp. 78–85.
- ¹¹A. H. Heuer, R. Caim, and V. Lantieri, *Acta Metall.* **35**, 661 (1987).
- ¹²T. Sakuma, *J. Mater. Sci.* **22**, 4470 (1987).
- ¹³M. Hillert and T. Sakuma, *Acta Metall. Mater.* **39**, 1111 (1991).
- ¹⁴S.-K. Chan, *Physica B & C* **150B**, 212 (1988).
- ¹⁵D. Fan and L.-Q. Chen, *J. Am. Ceram. Soc.* **78**, 769 (1995).
- ¹⁶Y. Ishibashi and V. Dvořák, *J. Phys. Soc. Jpn.* **58**, 4211 (1989).

- ¹⁷J. Katamura and T. Sakuma, J. Am. Ceram. Soc. **80**, 2685 (1997).
- ¹⁸X. Gonze and C. Lee, Phys. Rev. B **55**, 10355 (1997).
- ¹⁹S. Baroni, S. de Gironcoli, A. D. Corso, and P. Giannozzi, Rev. Mod. Phys. **73**, 515 (2001).
- ²⁰K. Kunk, in *Electronic Structure, Dynamics and Quantum Structural Properties of Condensed Matter*, edited by J. T. Devreese and P. van Camp (Plenum, New York, 1985), p. 227.
- ²¹W. Frank, C. Elsässer, and M. Fähnle, Phys. Rev. Lett. **74**, 1791 (1995).
- ²²K. Parlinski, Z.-Q. Li, and Y. Kawazoe, Phys. Rev. Lett. **78**, 4063 (1997).
- ²³S. Wei, C. Li, and M. Y. Chou, Phys. Rev. B **50**, 14587 (1994).
- ²⁴K. Karch, P. Pavone, W. Windl, O. Schütt, and D. Strauch, Phys. Rev. B **50**, 17054 (1994).
- ²⁵C. Lee and X. Gonze, Phys. Rev. B **51**, 8610 (1995).
- ²⁶G.-M. Rignanese, J.-P. Michenaud, and X. Gonze, Phys. Rev. B **53**, 4488 (1996).
- ²⁷A. A. Quong and A. Y. Liu, Phys. Rev. B **56**, 7767 (1997).
- ²⁸P. Söderlind and J. A. Moriarty, Phys. Rev. B **57**, 10340 (1998).
- ²⁹J. Xie, S. de Gironcoli, S. Baroni, and M. Scheffler, Phys. Rev. B **59**, 965 (1999).
- ³⁰J. Xie, S. P. Chen, J. S. Tse, S. de Gironcoli, and S. Baroni, Phys. Rev. B **60**, 9444 (1999).
- ³¹B. B. Karki, R. M. Wentzcovitch, S. de Gironcoli, and S. Baroni, Science **286**, 1705 (1999).
- ³²B. B. Karki, R. M. Wentzcovitch, S. de Gironcoli, and S. Baroni, Phys. Rev. B **61**, 8793 (2000).
- ³³P. Piekarczyk, P. T. Jochym, K. Parlinski, and J. Łażewski, J. Chem. Phys. **117**, 3340 (2002).
- ³⁴A. R. Oganov and P. I. Dorogokupets, Phys. Rev. B **67**, 224110 (2003).
- ³⁵P. Pavone, S. Baroni, and S. de Gironcoli, Phys. Rev. B **57**, 10421 (1998).
- ³⁶K. Persson, M. Ekman, and G. Grimvall, Phys. Rev. B **60**, 9999 (1999).
- ³⁷K. Gaár-Nagy, A. Bauer, M. Schmitt, K. Karch, P. Pavone, and D. Strauch, Phys. Status Solidi B **211**, 275 (1999).
- ³⁸K. Parlinski and M. Parlinska-Wojtan, Phys. Rev. B **66**, 064307 (2002).
- ³⁹Z. Łodziana and K. Parlinski, Phys. Rev. B **67**, 174106 (2003).
- ⁴⁰B. B. Karki and R. M. Wentzcovitch, Phys. Rev. B **68**, 224304 (2003).
- ⁴¹G. Kresse and J. Furthmüller, Phys. Rev. B **54**, 11169 (1996).
- ⁴²G. Kresse and J. Furthmüller, Comput. Mater. Sci. **6**, 15 (1996).
- ⁴³W. Kohn and L. J. Sham, Phys. Rev. **140**, A1133 (1965).
- ⁴⁴Y. Wang and J. P. Perdew, Phys. Rev. B **44**, 13298 (1991).
- ⁴⁵P. E. Blöchl, Phys. Rev. B **50**, 17953 (1994).
- ⁴⁶H. J. Monkhorst and J. D. Pack, Phys. Rev. B **13**, 5188 (1976).
- ⁴⁷X. Zhao and D. Vanderbilt, Phys. Rev. B **65**, 075105 (2002).
- ⁴⁸N. Igawa, Y. Ishii, T. Nagasaki, Y. Morii, S. Funahashi, and H. Ohno, J. Am. Ceram. Soc. **76**, 2673 (1993).
- ⁴⁹C. J. Howard, R. J. Hill, and B. E. Reichert, Acta Crystallogr., Sect. B: Struct. Sci. **44**, 116 (1988).
- ⁵⁰F. Detraux, P. Ghosez, and X. Gonze, Phys. Rev. Lett. **81**, 3297 (1998).
- ⁵¹G.-M. Rignanese, F. Detraux, X. Gonze, and A. Pasquarello, Phys. Rev. B **64**, 134301 (2001).
- ⁵²S. Fabris, A. T. Paxton, and M. W. Finnis, Phys. Rev. B **61**, 6617 (2000).
- ⁵³G. Kresse, J. Furthmüller, and J. Hafner, Europhys. Lett. **32**, 729 (1995).
- ⁵⁴A. P. Mirgorodsky, M. B. Smirnov, and P. E. Quintard, J. Phys. Chem. Solids **60**, 985 (1999).
- ⁵⁵C. Pecharromán, M. Ocaña, and C. J. Serna, J. Appl. Phys. **80**, 15 (1996).
- ⁵⁶H. Zhang, Y. Liu, K. Zhu, G. Siu, Y. Xiong, and C. Xiong, J. Phys.: Condens. Matter **11**, 2035 (1999).
- ⁵⁷T. Hirata, Phys. Rev. B **50**, 2874 (1994).
- ⁵⁸T. Merle, R. Guinebreteiere, A. Mirgorodsky, and P. Quintard, Phys. Rev. B **65**, 144302 (2002).
- ⁵⁹P. Bouvier and G. Lucazeau, J. Phys. Chem. Solids **61**, 569 (2000).
- ⁶⁰N. Kjerulf-Jensen, R. W. Berg, and F. W. Poulsen, in *Proceedings of the Second European Solid Oxide Fuel Cell Forum*, edited by B. Thorstensen (European Fuel Cell Forum, Switzerland, 1996), Vol. 2, p. 647.
- ⁶¹P. E. Quintard, P. Barbéris, A. P. Mirgorodsky, and T. Merle-Méjean, J. Am. Ceram. Soc. **85**, 1745 (2002).
- ⁶²C. Carlone, Phys. Rev. B **45**, 2079 (1992).
- ⁶³M. Ishigame and T. Sakurai, J. Am. Ceram. Soc. **60**, 367 (1977).
- ⁶⁴A. A. Maradudin, E. W. Montroll, G. H. Weiss, and I. P. Ipatva, *Theory of Lattice Dynamics in the Harmonic Approximation*, 2nd ed. (Academic, New York, 1971).
- ⁶⁵J. P. Poirier, *Introduction to the Physics of the Earth's Interior*, 2nd ed. (Cambridge University Press, New York, 2000).
- ⁶⁶S.-K. Chan, Y. Fang, M. Grimsditch, Z. Li, M. V. Nevitt, W. M. Robertson, and E. S. Zouboulis, J. Am. Ceram. Soc. **74**, 1742 (1991).
- ⁶⁷As a result of calculation with taking into account Born effective charges quoted from Ref. 51, errors of specific heat (ΔC_V), entropy (ΔS), and Helmholtz free energy (ΔF) in t -ZrO₂ are calculated to be 0.01 J/K mol, 0.25 J/K mol and 4 meV per formula unit at 1300 K, respectively. These errors are negligible in this study.